Synthesis and Photocatalytic Performance of TiO_2-CNT and Magnetized Fe_3O_4-TiO_2-CNT Multifunctional Hybrids: A Pickering Emulsion Platform for Organic Degradation

Written by

Erica Mason

Advised by

Dr. Navid Saleh

Second reader

Dr. Kerry Kinney

Submitted to

Megan McFadden

Engineering Honors Program Coordinator

McKetta Department of Chemical Engineering

And

Department of Civil, Architectural, and Environmental Engineering

The University of Texas at Austin

Spring 2018

Acknowledgements

I would like to thank those who gave me the opportunity to pursue an undergraduate thesis and who taught me how to work in a lab and conduct research. Firstly, I want to thank my adviser, Dr. Navid Saleh, who has mentored me for the last 3 years, and has constantly inspired me to pursue impactful research. I want to thank Dr. Kerry Kinney for being my second reader, and for working with me as a sophomore to find a research lab. I also want to thank Indu, who has mentored me in the lab, helped me begin my project as a sophomore, and has always aided me with my experiments. I want to thank the past and current members of the Saleh lab, especially Dipesh, Stetson, Craig, and Sneha, for patiently answering questions and assisting with my project. Additionally, I am grateful for Cindy and Alyssa who have helped me with my experiments over the last semester, and gave me the opportunity to teach others how to conduct research. Finally, I want to thank Dr. Zhou, Zongyao, Kyle, Rei, Shouliang, and Karalee for helping me with characterization.

Outside of the lab, I want to thank UT Austin and my professors for teaching me the skills necessary to pursue independent research, encouraging me to question the world around me, and for challenging me to make the world a better place. I want to thank my parents for their support throughout college, and especially my dad for introducing me to science and allowing me to work in his lab in high school.

Abstract

The oil and textile industries produce billions of gallons of wastewater containing toxic, and sometimes carcinogenic or mutagenic, chemicals that often disperse throughout wastewater as suspended oil droplets. Photocatalytic degradation is a promising method for organic degradation, but needs to be improved. Tuning the photo-activity of a photocatalyst, enhancing the reactor design, and ensuring a facile method to remove the photocatalysts from the purified wastewater will help photocatalysis become a realistic option for use in advanced water treatment plants. Thus, this study set out to engineer an efficient and reusable method to degrade dispersed organic chemicals, by combining the photocatalytic properties of titania (TiO_2), the electronic and hydrophobic properties of carbon nanotubes (CNTs), the magnetic abilities of iron oxide magnetite (Fe_3O_4), and the novel reactor design of Pickering emulsions. In this study, CNTs were magnetized with Fe_3O_4 and hybridized with TiO_2 following a sol-gel method in order to form magnetic Fe_3O_4-TiO_2-CNTs, to be used to stabilize Pickering emulsions to quickly degrade organic materials.

The metal oxide CNT hybrids were characterized for structure and magnetic behavior. Transmission electron microscopy (TEM) was used to assess hybridization of the CNTs. Scanning transmission electron microscopy (STEM) and energy dispersive spectroscopy (EDS) showed the elemental mapping of the metal oxide hybrids, displaying the presence of oxygen, iron, and titanium on the CNTs. X-ray diffraction (XRD) of the Fe_3O_4-CNTs displayed peaks due to graphite and magnetite structural planes as expected, and the Fe_3O_4-TiO_2-CNTs displayed peaks corresponding to the planes of graphite, magnetite, and titania anatase. Further XRD characterization is necessary, as several other peaks likely from other iron oxide structures were

also present on the spectra. The magnetic behavior of the Fe_3O_4-TiO_2-CNTs was also evaluated qualitatively, by viewing the movement of the hybrids on a magnetic stir plate.

Fe_3O_4-TiO_2-CNTs and TiO_2-CNTs were both used to successfully form Pickering emulsions, with droplets approximately 10 μm^2 in size. Although further study is necessary to analyze the degradation abilities, as well as retrievability and reusability of the Fe_3O_4-TiO_2-CNTs, the TiO_2-CNTs were used successfully to enhance photocatalytic organic degradation of Sudan III.

Contents

List of Figures

List of Tables

1. Introduction

1.1 Overview

The oil and textile industries produce billions of gallons of wastewater daily.[1] Hydraulic fracking utilizes large amounts of water that is prone to contamination with BTEX (benzene, toluene, ethylbenzene, and xylene) compounds, while textile industries release some 30% of utilized dyes, such as Sudan III, into wastewater streams.[1,2,3] Benzene and possibly ethylbenzene are carcinogenic, and are likely mutagenic, while all four BTEX compounds and many dyes are toxic.[4,5] The large amount of wastewater produced makes it challenging for treatment plants to manage the chemical waste, and these contaminants can get released into the natural environment.[1,6,7,8] Removal of organic contaminants and dye molecules from water is thus imperative.

Photocatalysis is a promising approach to degrade organic chemicals and dyes into nonhazardous products.[2,6,7,8,9,10] Titanium dioxide (TiO_2) is a commonly used photocatalyst due to its favorable band gap (3.2 eV), organic oxidation ability, and low cost.[7,9] TiO_2 and other photocatalysts have been added to carbon nanotubes (CNTs) in order to improve the reactive properties of the photocatalyst.[10] CNTs can facilitate electron storage and aid electron movement and charge separation, which can improve the photocatalytic degradation rate of TiO_2.[10,11] Magnetizing the CNTs is also possible, and could provide a simple way to retrieve and reuse materials.[12,13]

Another approach to improve photocatalytic degradation rates is to bring the target contaminants into close vicinity of the photocatalysts. In cases of non-miscible organic compounds (e.g., xylene, one of the compounds in the BTEX family), interactions between the catalysts and the target molecules can be increased by localizing the catalysts onto organic-water

interfaces. Such localization can only be beneficial if the particles can serve as emulsifiers and can stabilize the organic (or oil) droplets in a continuous medium of water, which is called a Pickering emulsion. Pickering emulsions are oil and water emulsions that are stabilized with particles (rather than surfactants) that localize at the oil-water interface and reduce surface tension to stabilize the droplets.[14,15] A Pickering emulsion effectively divides the oil phase into small droplets, bringing the photocatalyst into direct contact with the oil. In most degradation studies, the catalyst is simply dispersed in the wastewater, which limits rendering photoactive action to the target compunds.[5,6,7] Pickering emulsions can theoretically increase degradation rates.[10] Utilizing nanoparticles with hydrophobic attributes (e.g., carbon nanotubes) can preferentially partition to oil-water interface and thus can facilitate formation of Pickering emulsions.[10]

Pickering emulsions prepared with titanium dioxide (TiO_2) have been shown to quickly degrade organic dyes, and incorporating carbon nanotubes (CNTs) has been demonstrated to further improve the degradation process.[2,10] Several groups have synthesized reusable magnetic-CNTs in order to remove chromium or arsenic from wastewater.[12,13,16,17] Recently, salicylic acid has successfully been degraded using photocatalytic-magnetic-activated carbon.[18] However, photocatalytic-magnetic-CNTs have not been used to-date, alone or in combination with Pickering emulsions to degrade organics.

Combining the major breakthroughs of past research, including photocatalytic-CNTs, Pickering emulsions, and magnetic materials, I hope to improve the degradation rate of organics, in an environmentally friendly way. By combining the photocatalytic-CNT and Pickering emulsion technologies, wastewater can theoretically be divided into many miniature reactors, that can efficiently degrade the unwanted organics much faster.[10] Incorporating magnetic

particles onto the photocatalysts can further improve utility and environmental friendliness, through retrieval and reuse of the nanomaterials.

In this study, TiO$_2$-CNTs and Fe$_3$O$_4$-TiO$_2$-CNTs are synthesized using a modified sol-gel method.[13,19] The Fe$_3$O$_4$-TiO$_2$-CNTs are characterized to evaluate the loading of the TiO$_2$ and magnetite, assess the magnetism of the prepared material, and analyze the effectiveness of emulsification in the formation of Pickering emulsions. Initial photo reactivity of the Pickering emulsion is demonstrated with TiO$_2$-CNTs and Sudan III dye. Further study will include analyzing the photo reactivity of the magnetized Fe$_3$O$_4$-TiO$_2$-CNTs and demonstrating the retrievability and reusability of the magnetized Fe$_3$O$_4$-TiO$_2$-CNTs in the degradation of xylene.

1.2 Objectives

- Synthesize magnetic and photocatalytic carbon nanotubes (Fe$_3$O$_4$-TiO$_2$-CNTs). Characterize the Fe$_3$O$_4$-TiO$_2$-CNTs with transmission electron microscopy (TEM), scanning transmission electron microscopy (STEM), and x-ray diffraction (XRD) to understand the structure of the nanomaterials and evaluate the amount of hybridization.
- Use the hybridized carbon nanotubes to prepare stable Pickering emulsions and evaluate the emulsion properties. Degrade organics (Sudan III and Xylene) using TiO$_2$-CNTs and Fe$_3$O$_4$-TiO$_2$-CNTs.
- Analyze the rate of degradation with Ultraviolet-visible spectroscopy (UV-vis).

1.3 Hypothesis

Magnetic and photocatalytic carbon nanotubes can form Pickering emulsions and can degrade immiscible organics and/or organic dye molecules effectively.

2. Background and Literature Review

2.1 Wastewater

Oil and gas are in high demand around the world for energy usage. Oil and gas production involves the production of large amounts of produced water.[1] Produced water is water that is contaminated with a mixture of organics, metals, other inorganic solids, and gases. In the oil drilling process, water is commonly injected into reservoirs below the ground that contain water and hydrocarbons.[20] While hydrocarbons are recovered that can be used for energy, 3 times more produced water is yielded, resulting in approximately 250 million barrels daily of new toxic, produced water.[20,21] The produced water is at times allowed to be discharged into the ocean or the environment.[20]

Produced water often contains BTEX chemicals among other organics, which can be toxic and/or carcinogenic.[4,5] Some of these hydrocarbons are dissolved in the water, but some are not. Thus, produced water has hydrocarbons dispersed throughout the water and contains many suspended oil droplets.[18,20] Freshwater animals suffer, as hydrocarbons are highly toxic to these animals.[4,18] Therefore, removing the oil droplets and hydrocarbons is vital. Unfortunately, technologies in many wastewater treatment plants currently cannot remove small oil particles that are suspended in the water.[20]

Fracking, another method to produce energy resources, also produces billions of gallons of wastewater yearly, while also pumping billions of pounds of chemicals into the ground.[20,21] These fracking chemicals are generally toxic, mutagenic, and even carcinogenic, and again include BTEX chemicals.[4,5,21] In Texas, in 2014, 15 billion gallons of the contaminated wastewater was produced by fracking.[21] The toxic water is sometimes discharged into streams or disposed into retention ponds from which the toxins can leak into the environment.[20,21] The

entrance of BTEX chemicals and other organics into the environment is hazardous to the environment and to human health.[4]
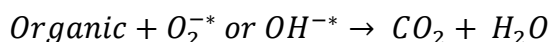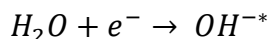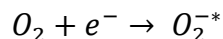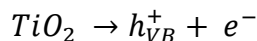
Textile industries also produce high amounts of toxic and carcinogenic water. There are approximately 100,000 different dyes, with complicated and varied structures, which can make dye degradation complicated.[22,23] Some dyes are water soluble, while others, such as Sudan III, are soluble in organics.[24] If the dyes are accidently released into the environment, or improperly degraded in treatment plants, the dyes can enter surface or groundwater, and harm flora and fauna. Many municipal water treatment plants are unable to remove dyes from the wastewater.[23] Thus, new technology is necessary to adequately treat the wastewater. Optimally, a method to treat both dyes, oils, and other chemicals found in wastewater is desirable.

2.2 Degradation Methods

Much research on water remediation and organic degradation has been conducted, including adsorption, filtration, evaporation, precipitation, electro dialysis, chemical oxidation, de-emulsifications, biological degradation methods, membrane systems, and photocatalytic degradation.[18] A combination of adsorption of organics using activated carbon and organoclay has been used to remove soluble and insoluble BTEX chemicals in water, but the method is unable to remove 100% of the organics and can be very expensive.[20,23] Chemical oxidation has been shown to degrade BTEX chemicals, but the process is energy intensive and the chemicals are costly.[20] The use of bacteria for anaerobic digestion to treat organics in wastewater is promising, as bacteria can be used to treat large amounts of organics. However, the efficiency and degradation ability is sensitive to temperature, pH, and the composition of the water.[24] Membrane filtration has the potential to produce highly pure streams, but often cannot produce

large amounts of a highly pure stream, and additionally produces a concentrated sludge that is not desirable.[20] Photocatalysis is an exciting option for degrading produced water from the oil industry. TiO_2 under UV light has been shown to destroy 90% of hydrocarbons in a water effluent vial in only 10 minutes.[20,25] Still, photocatalytic degradation must be made faster to be realistically implemented.[2,7]

Due to the promising nature of photocatalytic degradation for the treatment of oil-contaminated wastewater, I decided to pursue photocatalysis. Photocatalytic degradation occurs when light hits a catalyst, and if the energy of the light is higher than the band gap of the catalyst, then an electron will be excited, leaving a hole behind.[11,26] The excited electron reacts with oxygen or water via an indirect pathway to produce reactive hydroxyl radicals.[26,27] With titania as the photocatalyst, the oxygen and hydroxyl radical formation reactions are shown below:

$$TiO_2 \rightarrow h_{VB}^+ + e^-$$

$$O_2 + e^- \rightarrow O_2^{-*}$$

$$H_2O + e^- \rightarrow OH^{-*}$$

$$Organic + O_2^{-*} \text{ or } OH^{-*} \rightarrow CO_2 + H_2O$$

The radicals will then react with an organic substance, oxidizing the unwanted organic into H_2O and CO_2.[26]

Photocatalytic degradation of organics gained interest in the late 1970s, and has since become a major research focus.[28] In 1977, Frank and Bard demonstrated the use of TiO_2 and other semiconductors to oxidize cyanide into non-harmful products.[29] In 1978, Kraeutler and Bard demonstrated that TiO_2 powder irradiated with a Hg-Xe lamp could be used to decompose carboxylic acids into alkanes.[30] More recently in 2005, Chatterjee, et al. used TiO_2 to photocatalyticly degrade organics in the presence of visible light, expanding the spectra of light

able to degrade organics.[31] In 2012, Sangkhun, et al. used tungsten doped TiO_2 to photocatalyticly degrade BTEX chemicals in their gaseous state, removing up to 100% of the unwanted chemicals.[32] Murgolo, et al., in 2015, combined TiO_2 and CNTs to photocatalyticly degrade pharmaceutical products, demonstrating the utility of nano-TiO_2 and demonstrating the wide range of chemicals that can be photocatalyticly degraded.[33] Many others have investigated the use of TiO_2 and other semiconductors to degrade dyes, including Nawaz, et al, Aarthi, et al, and Nagaveni, et al.[2,7,9,11,15,22,23,34] There have been many studies altering the structure and composition of photocatalysts, new methods to synthesize photocatalysts, and different experimental designs to improve or vary the degradation ability of the materials. However, the material design can and should still be improved.

Photocatalytic reactors also need to be improved. Typical photocatalytic reactors either involve the catalysts being plated on the reactor walls, or a slurry reactor, in which small particles of the catalytic material are dispersed throughout the reactor.[35,36] The plated reactors have low surface area to volume of catalyst ratios, and the catalyst is often far from the organic pollutants.[35] The organic pollutant must be near the catalyst, or degradation is unlikely to occur.[10] Slurry reactors bring the catalysts closer to the pollutants, though proximity could still be improved.[10,36] Additionally, the catalyst must be able to be removed from the slurry reactor. Removing small, potentially nano-sized catalysts, is expensive and difficult.[13] Thus, for realistic implementation, the reactor design must also be improved.

2.3 Nanomaterials

TiO_2 has received the most attention for photocatalytic degradation as it is readily available, relatively cheap, inert chemically and biologically, non-toxic, hydrophilic, can produce

large amounts of reactive oxygen species (ROS), and has good photostability.[9,28,37,38] TiO_2 has two important crystalline structures that are photoreactive: rutile and anatase. While both structures have ideal band-gaps, anatase is more reactive photocatalyticly.[26,28] For TiO_2 with the anatase crystalline structure, the band gap is 3.2 eV. Thus, light with at least an energy of 3.2 eV, corresponding to a wavelength below 388 nm, will be able to excite TiO_2 and enable photocatalytic activity.[26,28] While other semiconductors have lower band gaps, stability and cost still make TiO_2 the most desirable.

Titania is photoreactive in bulk- and nano-form. Nanomaterials have become of increasing importance across a vast array of industries, due to the ability to fine tune both their electronic and surface properties.[19] Many studies have altered the size and tuned the properties of TiO_2 anatase to improve the reactivity and lower the cost of the material. In 2001, Sokmen, et al. showed TiO_2 doped with Ag lowered the band gap of the material and increased the rate of photocatalytic degradation.[39] Nagaveni, et al. demonstrated the increased degradation rate for nano-sized TiO_2.[9] Kyoung-hwa, et al. demonstrated the ability to hybridize CNTs with TiO_2, and how the CNTs encourage electron movement and facilitate electron storage and charge separation.[10,11,40]

Like TiO_2, CNTs have also received a lot of attention. Although Bacon, et al. may have produced CNTs in the 1970s, the importance of CNTs didn't expand until the early 1990s, when Iijima, et al. synthesized and imaged CNTs.[41,42] CNTs have since revolutionized science. CNTs have the structure of graphene sheets that have been rolled and can exist as single or multiwalled sheets. They typically have a diameter between 10 and 100 nm, giving them a high surface area to volume ratio.[19] CNTs have high strength and flexibility due to their carbon-carbon bond make up.[41] The carbon-carbon bonds also make CNTs electrically conductive and hydrophobic.[10,39]

The size and structure of CNTs give them unique optoelectronic, thermal, and mechanical properties, making CNTs useful in a variety of applications.[19] Additionally, CNTs can easily be hybridized with metals and semiconductors, further expanding their utility.

Due to the rolled graphene structure of CNTs, the carbons can easily be oxidized to form hydroxyl and carboxylic groups on the tubes.[41] The hydroxyl and carboxylic groups are vital for the hybridization ability of CNTs. CNTs can be hybridized with TiO_2, producing a nanomaterial with the beneficial properties of both CNTs and TiO_2, and new properties. Hybridizing TiO_2 onto CNTs decreases the band gap of TiO_2, improving the photocatalytic activity of the material.[19] Hybridized CNTs may also lead to higher production of radicals, vital to the photodegradation process.[43]

Although CNTs and TiO_2 have a promising future in water treatment, the materials must be able to be separated from the treated wastewater. Due to the nano-size of the materials, filtration is costly and largely ineffective. A simple method to remove the materials is with magnetism. CNTs can be magnetized by hybridizing the CNTs with iron oxide. Cunha, et al, Gupta, et al., and Luo, et al. have synthesized magnetic CNTs by hybridizing them with iron oxide.[12,13,16] Luo, et al. has additionally hybridized the magnetic CNTs with MnO, for chromium removal applications.[13] Zhu, et al. has synthesized CNTs with TiO_2 on the outer shell and iron oxide on the inside of the tube.[44] Synthesizing CNTs hybridized with TiO_2 and iron oxide for water treatment applications has not been researched, as far as I can tell.

2.4 Pickering Emulsions

Photodegradation rates can be improved by tuning the catalysts, and by bringing the undesirable chemicals closer to the catalysts. In produced water from oil production, small oil

droplets are dispersed throughout the wastewater.[20] As discussed, in many water treatment studies, photocatalysts are simply dispersed within the wastewater.[6,7,9,11] With the materials dispersed, the photocatalysts may not be near to all of the oil droplets.

A Pickering emulsion is a mixture of oil and water that is stabilized by small, solid particles, in place of surfactants. The particles must be amphoteric in order to hold the two immiscible phases together and stabilize an emulsion.[14] The solid particles will ideally sit at the interface of the oil and water surfaces, creating small spheres with high surface area, which act as individual photocatalytic reactors. Thus, in a Pickering emulsion, the photocatalysts are in direct contact with the oil that they are degrading, which should speed up the degradation rate. Figure 1 shows an example oil droplet in red, surrounded by tiny particles containing TiO_2 on the blue edge of the sphere. The photocatalytic degradation process is also shown, with UV light excited electrons on the TiO_2, producing hydroxyl radicals which react with and degrade the undesired organics.[25,26]
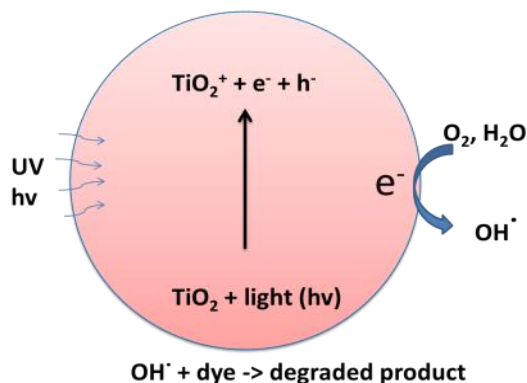

Figure 1. Photocatalytic degradation pathway on a Pickering emulsion droplet

Several groups have successfully used Pickering emulsions to degrade dyes, including Zhai, et al., who used Ag_3PO_4 and multiwalled CNTs (MWCNTs) dispersed in a water in oil Pickering emulsion to photocatalytic degrade a water soluble dye, and Nawaz, et al. who used SA-

TiO$_2$ as a Pickering emulsion to degrade an aqueous dye.[2,10,15] Additionally, Wu, et al. has used Pickering emulsions to degrade nitrobenzene.[8] As far as I know, however, Pickering emulsions have not been combined with CNTs hybridized with TiO$_2$, iron oxide, or both, for use in degrading organics.

3. Materials and Methods

3.1 Materials

Pristine multiwalled carbon nanotubes (MWCNTs, O.D. 8-15 nm) were purchased from Cheap Tubes Inc. (Brattleboro, VT). Titanium (IV) isopropoxide (TTIP), concentrated sulfuric acid, cyclohexane, and Sudan III from Sigma Aldrich (ST. Louis, MO) were used. Isopropanol, ammonium hydroxide, and ferric chloride hexahydrate were purchased from Fisher Scientific (Pittsburgh, PA). Ferrous chloride tetrahydrate from ACROS/ORGANCIS (New Jersey) was used. Throughout the experiments, 18.2 mΩ (Milli-Q) water was utilized.

3.2 Synthesis and Characterization of Fe$_3$O$_4$-TiO$_2$-CNTs

3.2.1 Functionalization of CNTs

Following the Das et al. method, 1 g of MWCNTs were purified via acid-etching through dispersion in 150 mL each of concentrated nitric and sulfuric acids. The solution was refluxed under stirring at 100 °C for 3 h under a nitrogen atmosphere, to remove impurities and oxidize the CNTs. Once cooled, the CNTs were filtered using PTFE 0.22 μm membranes and washed with DI water, until the solution was no longer acidic. After drying the CNTs in a desiccator, the CNTs were ground with mortar and pestle.[19]

3.2.2 Synthesis of TiO₂-CNTs

Again using the elegant Das et al. method and adaptations of the method, the CNTs and Fe_3O_4-CNTs were hybridized with titania. 100 mg of CNTs, or Fe_3O_4-CNTs, were dispersed in 100 mL of isopropanol. While the CNT solution was under reflux, purged with nitrogen, and stirred at 80 °C, a solution of 84.33 μL of TTIP dispersed in isopropanol was added at 0.301 mL/min to the solution using a peristaltic pump (Ismatec, Wertheim, Germany). After 3 h of reflux, the pump was again used to add 1.67 mL of DI water at 0.301 mL/min to the dispersion, and the system refluxed for another hour. The solution was then dried over a hot plate, and the remaining solids were ground. The hybridized CNTs were finally calcined in a furnace at 400 °C in a nitrogen atmosphere, to cause the titania phase transformation to anatase.[19]

3.2.3 Synthesis of Fe₃O₄-TiO₂-CNTs

The CNTs and TiO₂-CNTs were magnetized using methods adapted from Cunha et al. and Luo et al. 20 mg of CNTs or TiO₂-CNTs were dispersed in 35 mL of DI water. 1 mL each of 0.2 M ferric chloride hexahydrate and 0.1 M of ferrous chloride tetrahydrate were added to the solution, which was subsequently heated to 70 °C. While stirring, 30 mL of 5M NH_4OH was added to the solution, to create a basic solution. After being stirred for 1.5 h at 70 °C, the solution was cooled. The CNTs were finally washed with a series of DI and ethanol using 0.22 μm PTFE filters, before being dried in an oven at 60 °C.[12,13] The synthesis process is shown graphically in Appendix A.

3.2.4 Characterization of Fe₃O₄-TiO₂-CNTs

The CNTs, TiO$_2$-CNTs, Fe$_3$O$_4$-CNTs, and Fe$_3$O$_4$-TiO$_2$-CNTs were characterized using transmission electron microscopy (TEM), JEOL 2010F high resolution transmission electron microscopy (HRTEM/STEM) with energy dispersive spectroscopy (EDS) (HRTEM, JEOL, Japan), and x-ray diffraction (XRD). For the TEM and HRTEM/STEM, the nanomaterials were dispersed in ethanol, and dropped onto carbon coated copper TEM grids (SPI Supplies, West Chester, PA). The magnetic character was analyzed qualitatively with a magnetic stir plate.

3.3 Preparation and Characterization of Pickering Emulsions

Pickering emulsions were synthesized with .7 mg TiO$_2$-CNTs or 2-5 mg of Fe$_3$O$_4$-TiO$_2$-CNTs dispersed in 20 mL of DI water by sonication for 10 min. In preliminary experiments, the oil phase consisted of Sudan III (0.25 mg/ml) dispersed in 6 mL of cyclohexane. For later experiments, 8 mL of xylene was used, with no dye added, for the oil phase. The CNT aqueous solution and the oil solutions were combined and sonicated for 40 minutes to create the Pickering emulsions. A control was created following the same method, in which no CNTs were added. The formation and stability of the Pickering emulsions were assessed with optical microscopy using a Nikon confocal microscope (Nikon Eclipse Ti-E, Nikon Instruments Inc., Melville, NY). The initial emulsions with dye were also analyzed with Cryo-EM (FEI Quanta 650 SEM).

3.4 Photocatalytic Activity

To analyze photoreactivity, the Pickering emulsions were irradiated with ultra-violet (UV) radiation at 253.7 nm in a photo-reactor (Rayonet RPR-100, Southern New England Ultraviolet, Branford, CT) for 60 minutes. UV-Visible Spectroscopy (UV-Vis) (Agilent 8454,

Santa Clara, CA) and direct visual observations were used to assess the degradation of the organics quantitatively and qualitatively.

4. Results

4.1 Structural Characterization

TEM images were taken of the Fe_3O_4-CNTs and the Fe_3O_4-TiO_2-CNTs. Figure 2 shows CNTs with magnetite attached to the surface of the CNTs, on a 100 nm and 50 nm scale. On non-hybridized CNTs, the surface would be clean, without any dense clusters. As can be seen in Figure 2, there are many dense clusters on the CNTs, showing that iron oxide has attached to the nanotubes. These clusters are not equally spaced, so the magnetization process may need improvement.
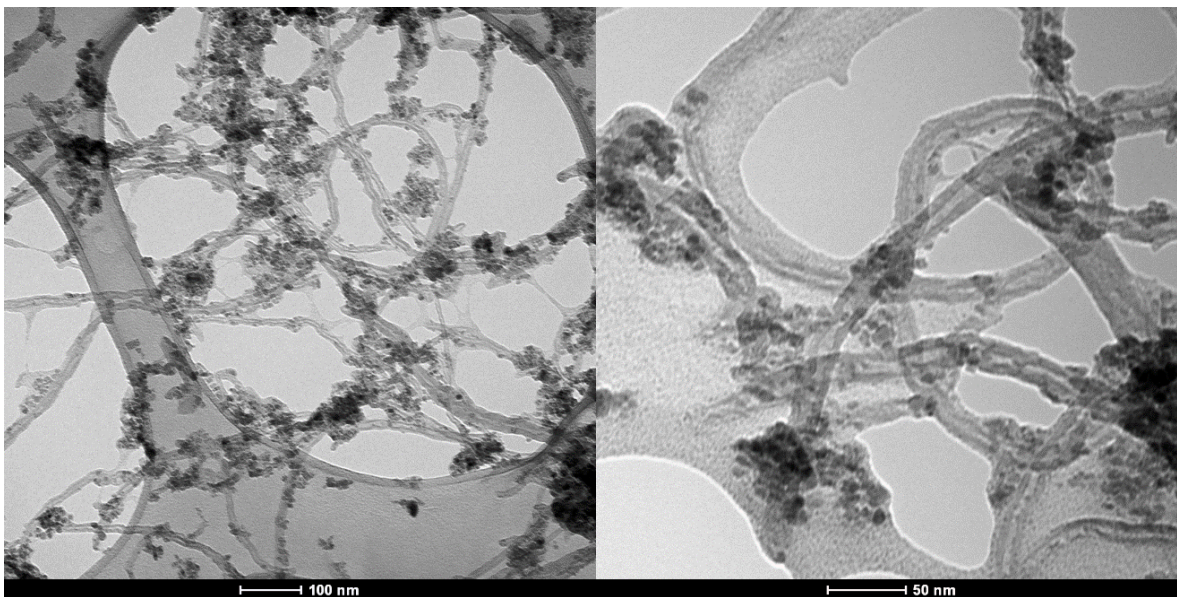

Figure 2. TEM images of Fe_3O_4-CNTs on a 100 nm scale (left) and a 50 nm scale (right).

Figure 3 shows TEM images of CNTs that have been magnetized and then hybridized with titania, on a 50 nm scale. The tubes have more clusters on them then the CNTs that had only

been magnetized, suggesting the tubes have successfully been hybridized with titania as well. The number of dense clusters on the CNTs are high, meaning many of the carboxylic and hydroxyl sites are full. The high amount of iron oxide and titania on the nanotubes may affect the hydrophobicity of the CNTs, so lower loading amounts may be necessary to form Pickering emulsions.
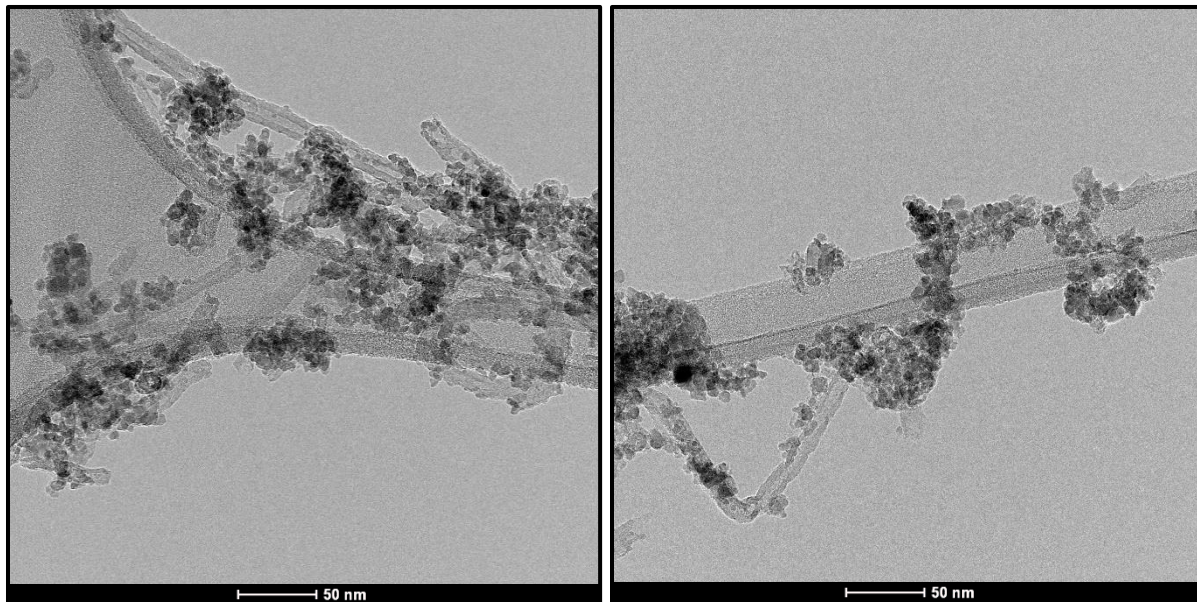

Figure 3. TEM images of Fe_3O_4-TiO_2-CNTs on 50 nm scales

To further assess the elemental composition of the CNTs, scanning transmission electron microscopy (STEM) was used to obtain electron micrograph images. Figure 4 shows the elemental distribution of the Fe_3O_4-TiO_2-CNTs. Carbon is displayed in red, oxygen is displayed in light blue, iron is displayed in green, and titanium is displayed in dark blue.
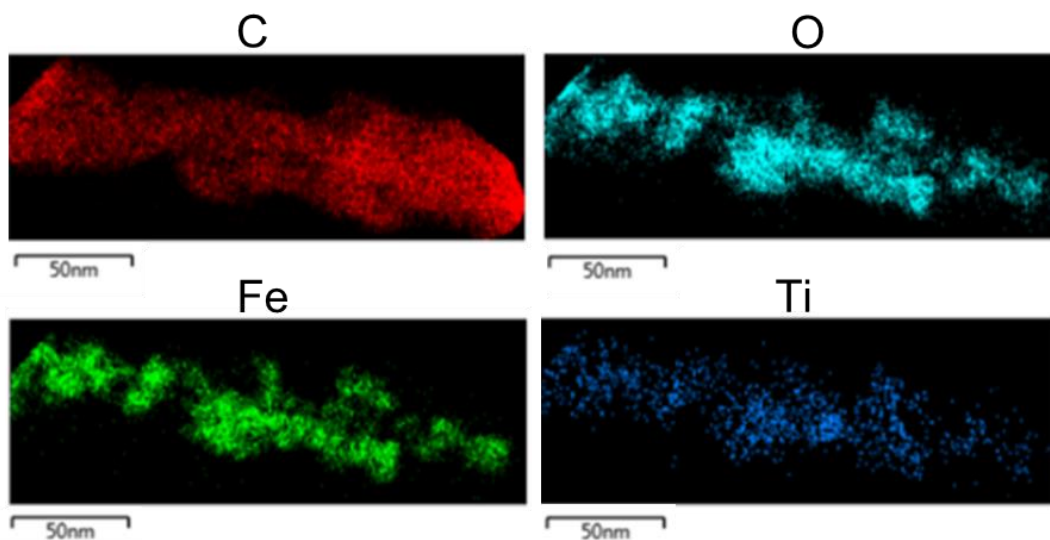
Figure 4. STEM images of Fe$_3$O$_4$-TiO$_2$-CNTs on 50 nm scales

Qualitatively, Figure 4 shows that the CNTs have high amounts of carbon and oxygen, large amounts of iron, and some titanium. The low amounts of titanium is a result of using the 1:30 loading, as described by Das, et al.[19] The quantitative elemental mapping results are shown in Table 1, and support the qualitative results. Increasing the loading of the titania may be necessary for photocatalytic ability.

Table 1. Elemental distribution of Fe$_3$O$_4$-TiO$_2$-CNTs

Element	Weight %
C	64.9
O	11.5
Ti	1.1
Fe	8.7

The crystal structure of the materials was assessed with XRD, shown in Figure 5. Iron oxide can have many different crystal strucutres, and not all of the structures are magnetic. Magnetite, Fe_3O_4, is a magnetic iron oxide structure and is typically formed between reactions of ferric and ferrous salts, so the goal was to form magnetite.[45] Figure 5 shows the diffraction patterns of Fe_3O_4-CNTs in green and Fe_3O_4-TiO_2-CNTs in black. CNTs have a characteristic peak due to the graphite structure at 26.14° corresponding to the (002) plane.[19] Magnetite, Fe_3O_4, has characteristic peaks at 30.25°, 35.69°, 43.25°, 53.8°, 57.37°, and 62.89°, corresponding to the (220), (311), (400), (422), (511), and (440) crystal planes.[13] In Figure 5, the CNT peak is shown by the red dotted line and the magnetite is shown by the green vertical lines. Both samples have definite peaks for the CNT peak and for most of the magnetite peaks. Thus, based on the TEM, HRTEM/STEM, and XRD, the samples are CNTs with Fe_3O_4 attached.
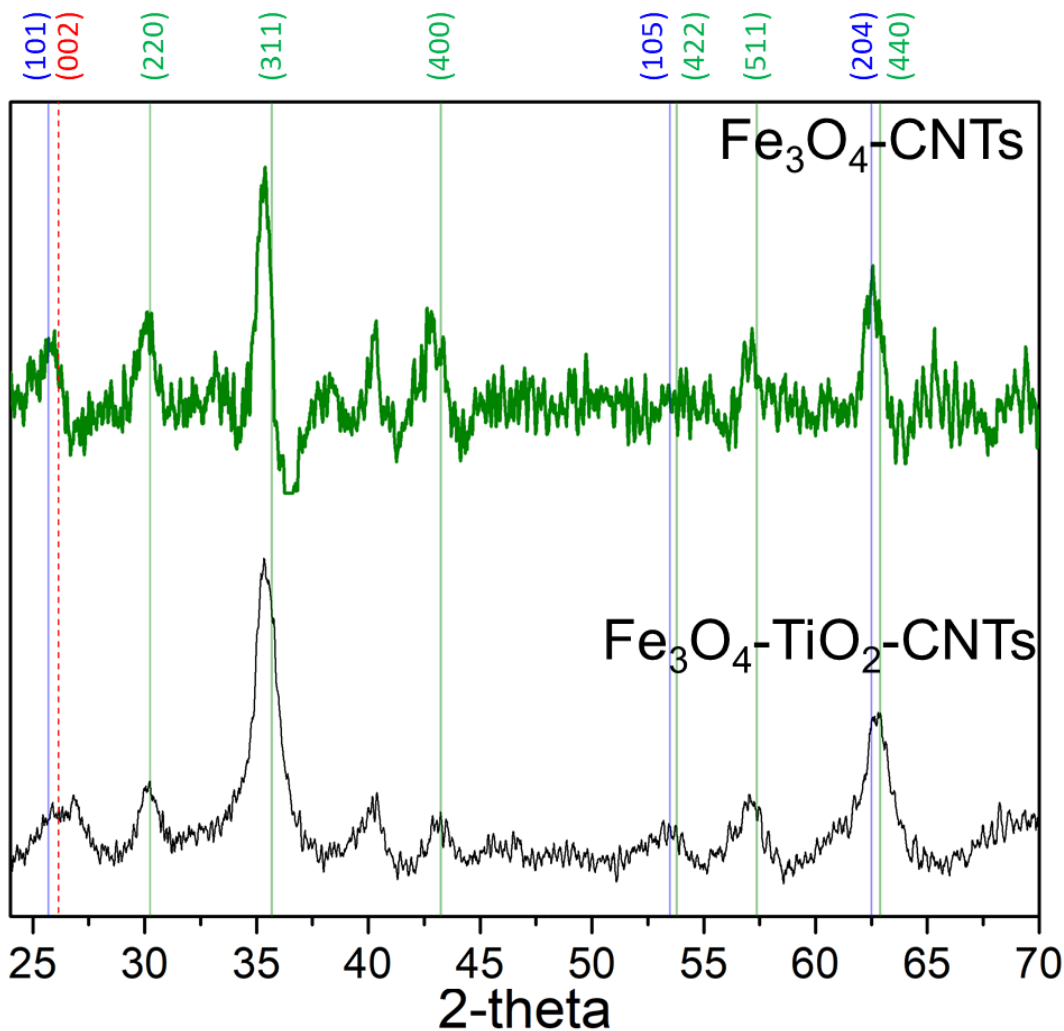
Figure 5. XRD spectra of Fe$_3$O$_4$-CNTs (green, top) and Fe$_3$O$_4$-TiO$_2$-CNTs (black, bottom)

The XRD pattern in Figure 5 also shows the typical peaks for TiO$_2$ anatase as the blue drop down lines. CNTs hybridized with TiO$_2$ display a peak around 25.7° most strongly and also show weaker peaks at 53.5° and 62.5°. These peaks are due to the presence of the (105) and (204) planes present in anatase.[19] As the TiO$_2$ loading for this sample was low, the XRD peaks are quite weak. However, the 25.7° peak is present, as seen with the widening of the peak around 26° in the Fe$_3$O$_4$-TiO$_2$-CNTs XRD pattern shown in Figure 5. There is also a weak anatase peak for the (105) plane present in the Fe$_3$O$_4$-TiO$_2$-CNTs XRD pattern, and a widened peak associated

with the (204) anatase and (440) magnetite planes.[19] Based on the XRD and HRTEM/STEM

patterns, I have successfully synthesized Fe_3O_4-TiO_2-CNTs, though the loading of the TiO_2 is

low.

4.2 Magnetic Characterization

The presence of magnetite shown by the XRD suggests that the nanomaterials should be

magnetic. However, the materials must be magnetic enough to be able to respond to a magnet.

Optimally, SQUID magnetometry would be used to develop magnetic hysteresis plots and

quantitatively assess the magnetic behavior. However, the SQUID was unavailable, so a

qualitative assessment was completed.

Figure 6. Movement of Fe_3O_4-TiO_2-CNTs on stir plate. Left: Initial. Right: After brief stir
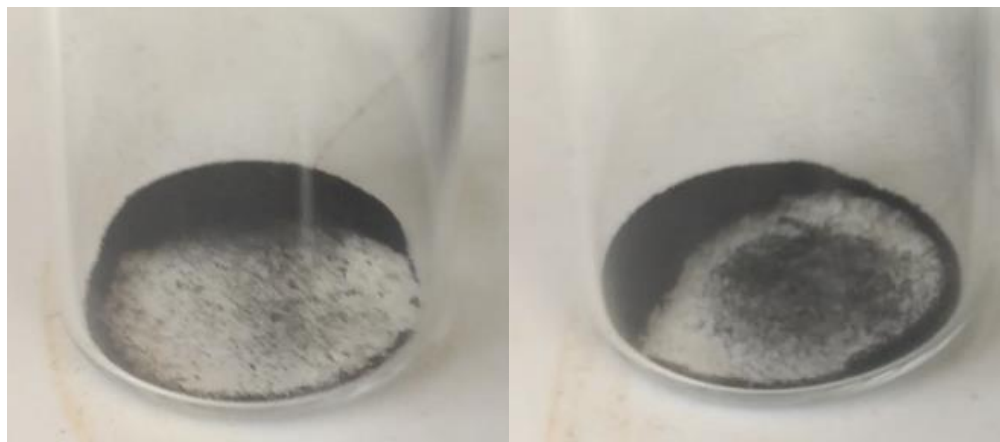
Figure 6.1 Movement of Fe_3O_4-TiO_2-CNTs on stir plate. Left: Initial. Right: After brief stir

To qualitatively evaluate the magnetic behavior of the synthesized materials, the samples were placed on a magnetic stir plate. Figures 6 and 6.1 show two samples of Fe_3O_4-TiO_2-CNTs on a stir plate. The images on the left in both figures show the location of the materials before the magnetic stir plate has been turned on. The images on the right in Figures 6 and 6.1 show the location after the stir plate has been turned on briefly. As can be seen, many of the CNTs have moved across the stir plate, demonstrating their magnetic behavior. After extended stirring, nearly all of the CNTs moved across the stir plate. When dispersed in water or ethanol samples, the Fe_3O_4-TiO_2-CNTs remain responsive to the magnetic stir plate.

4.3 Pickering Emulsion Characterization

Although TiO_2-CNTs are not the focus of this present study, their emulsification and photocatalytic properties are expected to be similar to that of their magnetized counterparts, the Fe_3O_4-TiO_2-CNTs. Thus, initial experiments completed with the TiO_2-CNTs that have not yet been completed with the Fe_3O_4-TiO_2-CNTs remain useful, and are analyzed in the Pickering emulsion characterization and the photocatalytic activity sections. Pickering emulsion

characterization was performed on Fe_3O_4-TiO_2-CNTs, but photocatalytic activity still needs to be assessed.

Preliminary Pickering emulsions were formed using both TiO_2-CNTs and Fe_3O_4-TiO_2-CNTs. The TiO_2-CNTs were used to emulsify cyclohexane and water, while the Fe_3O_4-TiO_2-CNTs were used to emulsify xylene and water. Images and confocal microscopy images of both emulsions are shown in Figure 7 and Figure 8.

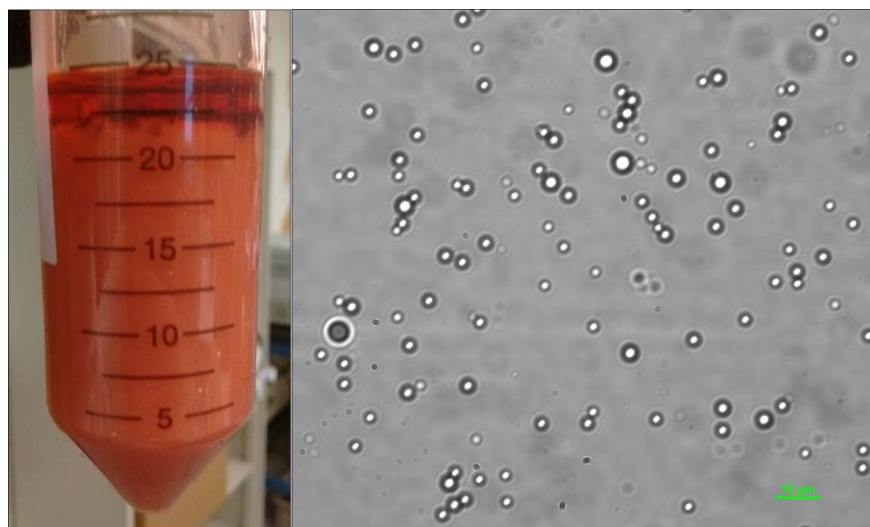Figure 7. Cyclohexane with Sudan III, DI, and TiO_2-CNT Pickering emulsion. Left: Pickering emulsion. Right: Confocal microscopy image
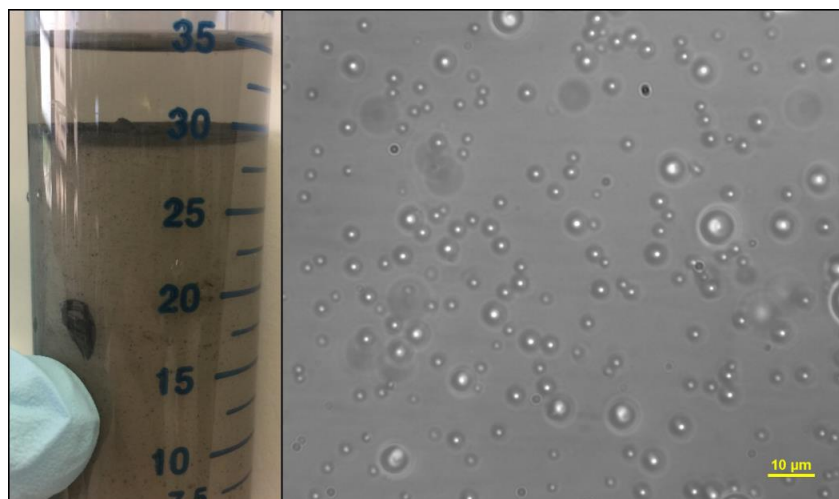
Figure 8. Xylene, DI, and Fe$_3$O$_4$-TiO$_2$-CNT Pickering emulsion. Left: Pickering emulsion. Right: Confocal microscopy image

In both Figures 7 and 8, the images on the left show the Pickering emulsions. In Figure 7, the Pickering emulsion is characterized by the light red, slightly foamy texture between 5 and 20 mL in the centrifuge tube. The region above 22 mL is cyclohexane that did not emulsify. At the very bottom of the centrifuge tube, a mostly water phase is present. This separation is typical of Pickering emulsions, with the emulsion being in the middle and pure phases above and below.[10,14] Likewise, in Figure 8, the region between 30 and 35 mL is mostly pure xylene, while the Pickering emulsion is in the region below 30 mL. The confocal images, droplet characterization, and degradation experiments were based on the Pickering emulsion portion only, avoiding the pure phase sections.

The confocal microscopy images in Figures 7 and 8 both show the Pickering emulsion droplets, with a scale bar of 10 μm. Confocal microscopy shows that an emulsion was formed, with droplets of one phase dispersed in the other phase. As no clusters of CNTs can be seen in the confocal images, the CNTs must be at the interphase of the oil and water phases, surrounding

the droplets. Although CNTs are nano in size, when clumped together, as they would be if not at the interphase, the clumps would be visible on this scale. Appendix B shows cryogenic electron microscopy (Cryo-EM) images showing the CNTs on the surface of the droplets, providing further evidence of the location of the CNTs.

The confocal images were further assessed for droplet size and quantity, as shown in Table 2. Mean represents the average area of a droplet, and standard deviation assesses the variety of droplet sizes. Quantity represents approximately how many droplets were present, on average, in equivalently sized confocal images at 40x magnification.

Table 2. Pickering Emulsion Droplet Size and Quantity Assessment

	TiO_2-CNTs	Fe_3O_4-TiO_2-CNTs
Mean (μm^2)	13.7	6.9
Standard Deviation	6.6	3.4
Quantity	200	300

As shown in Table 2, the average size of the Pickering emulsions formed with the TiO_2-CNTs was about twice the size of the Pickering emulsions formed with the Fe_3O_4-TiO_2-CNTs. The difference in size may be due to the difference in organic chemical used, the difference in the surface characteristics of the CNT hybrids, and the time between emulsification and characterization. The Fe_3O_4-TiO_2-CNT Pickering emulsion was assessed immediately, whereas the TiO_2-CNT Pickering emulsion was assessed after 1.5 hours. These initial results show that emulsions can be formed with both hybrids and with different organic chemicals, to form droplets around 10 μm^2 in size. As each droplet is ideally surrounded by CNTs forming a reactor, each reactor is effectively micron size, which should lead to quick degradation rates. The large

number of droplets in each image is also promising for quick degradation, as many droplets correlates to more reactors.

The standard deviation of the TiO_2-CNT stabilized Pickering emulsion was also about twice that of the Fe_3O_4-TiO_2-CNT stabilized Pickering emulsion. In both Pickering emulsions, the standard deviation was about half of the mean droplet size, which was expected based on literature results.[14] The droplets do not vary greatly in size.

4.4 Photocatalytic Ability

The photoactivity experiments for the Fe_3O_4-TiO_2-CNTs still need to be completed, but preliminary reactivity experiments with the TiO_2-CNTs have been completed. The TiO_2-CNTs are expected to have a slightly better reactivity than the Fe_3O_4-TiO_2-CNTs, as the TiO_2 loading on the TiO_2-CNTs was 3 times higher. Still, similar reactivity trends are expected.

A Pickering emulsion consisting of cyclohexane, Sudan III red dye, and water, stabilized with TiO_2-CNTs, was irradiated with UV-light for 60 minutes. The degradation was assessed based on color loss, as shown in Figure 9. Figure 9 also shows the degradation of the control, which consisted of cyclohexane, Sudan III red dye, and water, with no stabilization material.
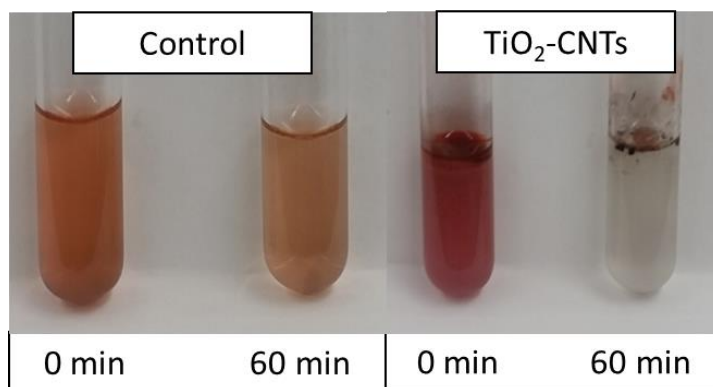

Figure 9. Photocatalytic degradation of Sudan III dye. Left: Control. Right: TiO_2-CNT Pickering emulsion

As can be seen in Figure 9, slight color loss has occurred in the control, while near complete color loss has occurred in the TiO_2-CNT Pickering emulsion. Thus, based on visual observation, the TiO_2-CNTs sped up the degradation process. The color loss of the control and the TiO_2-CNT Pickering emulsion were further characterized with UV-vis, as shown in Figure 10.
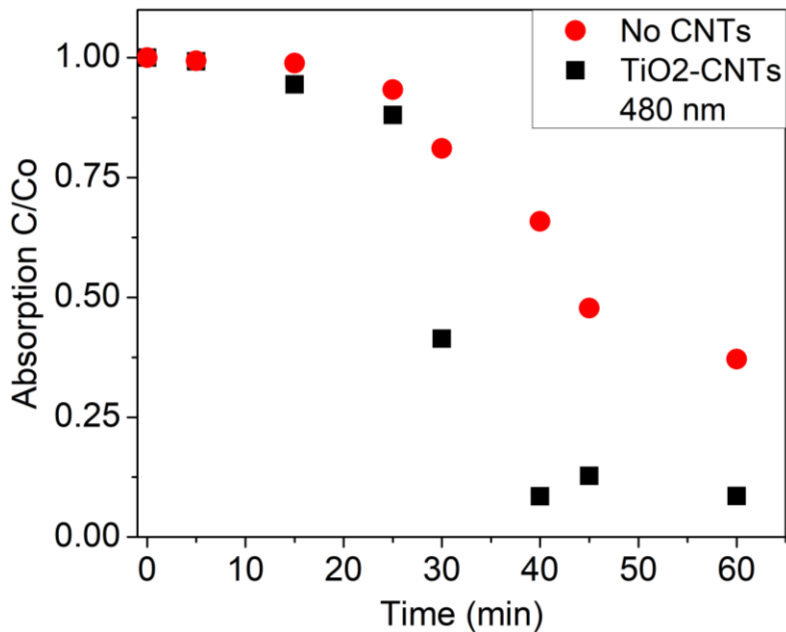

Figure 10. Concentration over initial concentration at various degradation time points, for the control (red) and the TiO_2-CNT Pickering emulsion (black). $\lambda = 480$ nm.

Figure 10 confirms the visual observation that the color disappeared much more rapidly in the wastewater solution containing TiO_2-CNTs than in the control solution. The TiO_2-CNTs clearly aided in the degradation of the organic dye, characterized by the loss of color. The degradation is again shown in Figure 11, across all absorption wavelengths.
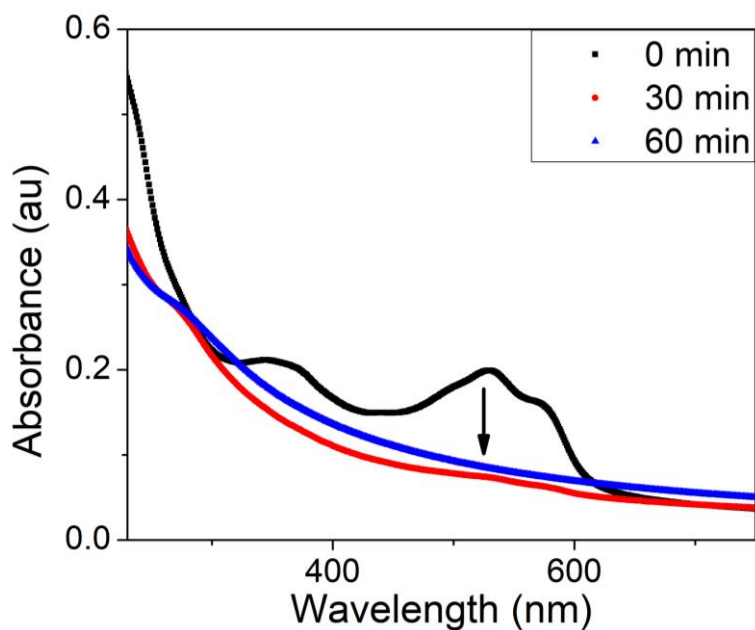
Figure 11. Absorbance across all wavelengths 200-750 nm, for a solution containing Sudan III and TiO$_2$-CNTs, at 3 different exposures times to UV-light.

Figure 11 shows the absorbance spectra of the Pickering emulsion containing cyclohexane, water, Sudan III, and TiO$_2$-CNTs, shown by the black line "0 min". The same solution was degraded under UV-light for 30 minutes and 60 minutes, and the resulting spectra are shown by the red and blue lines, respectively. All of the peaks present at 0 minutes of irradiation disappeared, showing the effect of the UV-light on the Sudan III structure.

The TiO$_2$-CNTs increased the speed of degradation of the organic dye. It is expected that the magnetic Fe$_3$O$_4$-TiO$_2$-CNTs will also degrade the organic dye quickly. Additionally, we expect that both TiO$_2$-CNTs and Fe$_3$O$_4$-TiO$_2$-CNTs will be able to degrade other organics, such as xylene. The degradation of xylene with Fe$_3$O$_4$-TiO$_2$-CNTs will be assessed in the future.

5. Conclusion

Magnetic Fe_3O_4-TiO_2-CNT hybrids have been successfully synthesized. Preliminary characterization results show that hybridization of the CNTs with both iron oxide (magnetite) and titania (anatase) was achieved, as determined by TEM, STEM, and XRD. The magnetic behavior of the Fe_3O_4-TiO_2-CNTs was demonstrated qualitatively using a magnetic stir plate. Pickering emulsions were also prepared with both the TiO_2-CNTs and Fe_3O_4-TiO_2-CNTs. Finally, the TiO_2-CNTs were successfully used to degrade an organic dye, which signifies that the Fe_3O_4-TiO_2-CNTs can also be an effective photocatalyst. The results from this study are promising, however, further work remains to evaluate the photocatalytic ability, retrievability, and reusability of the Fe_3O_4-TiO_2-CNTs.

6. Appendix

Appendix A: Synthesis of Fe_3O_4-TiO_2-CNTs

The synthesis of Fe_3O_4-TiO_2-CNTs is shown in Figures 12 and 13. The order of hybridization with Fe_3O_4 and TiO_2 can be done in either order, adding the of Fe_3O_4 or TiO_2 first. Magnetizing the CNTs first was the chosen protocol, however, and is displayed in Figures 12 and 13. Figure 12 illustrates the magnetization of functionalized-CNTs to form magnetic Fe_3O_4-CNTs. Figure 13 illustrates the hybridization of the Fe_3O_4-CNTs with titanium isopropoxide to form the Fe_3O_4-TiO_2-CNTs. Figures 12 and 13 were adapted from Das, et al.
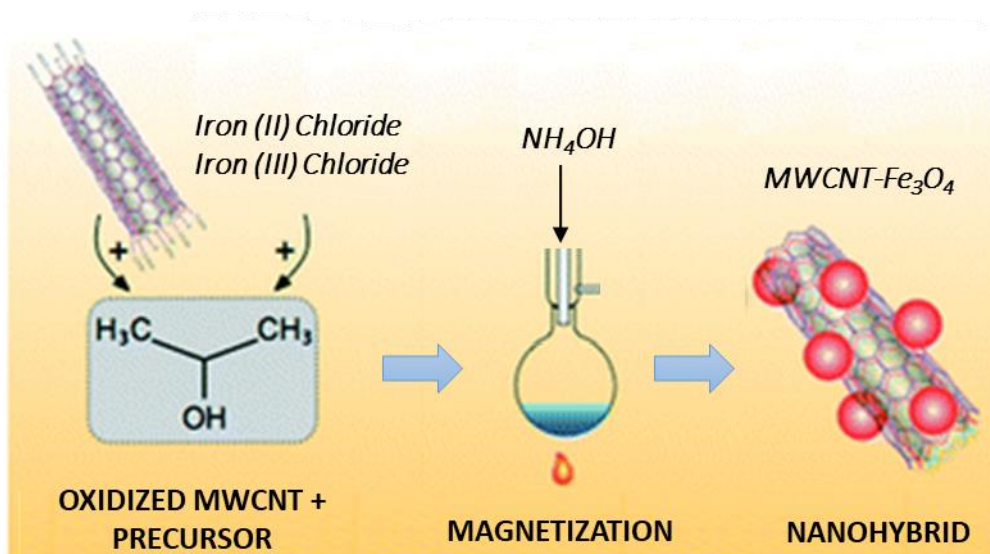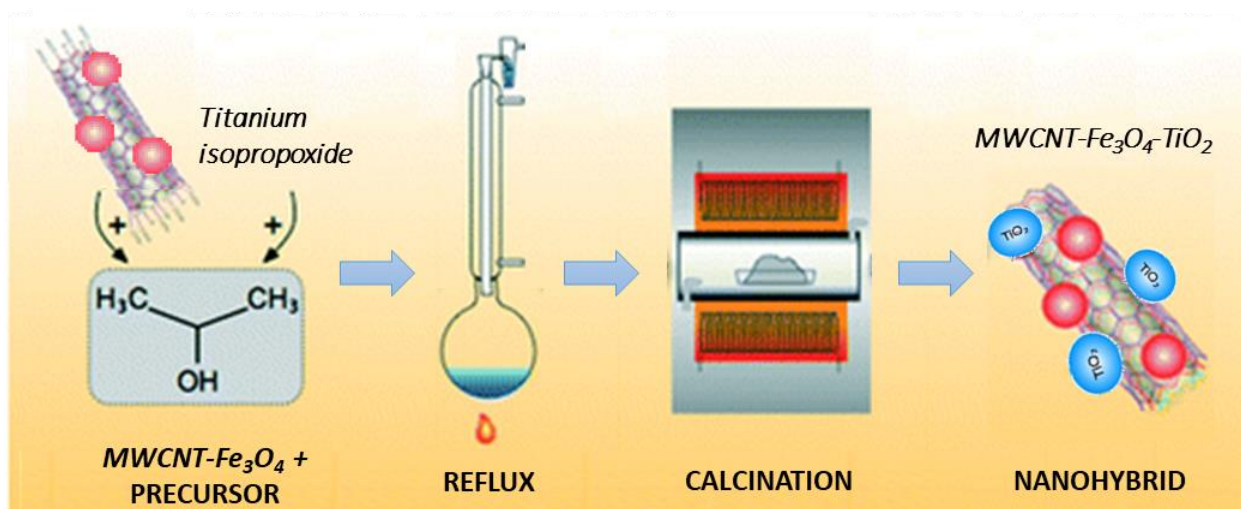

Figure 12. Magnetization of CNTs

Figure 13. Hybridization of Fe_3O_4-CNTs to form Fe_3O_4-TiO_2-CNTs

Appendix B: Cryo-EM TiO₂-CNTs Pickering emulsion Assessment

To observe the surface morphology of the Pickering emulsion, where the CNTs are hypothesized to surround the organic phase, Cryo-EM images were taken, as seen in Figure 14, with the control on the left and the TiO_2-CNT Pickering emulsion on the right. Spherical structures can be seen in both images. However, the images of the Control on the left appear to have a smooth surface while the TiO_2-CNT Pickering emulsion sample on the right has a bumpy surface, resembling Brussel sprouts. The bumps are likely the nanotubes wrapping around the surface of the organic.
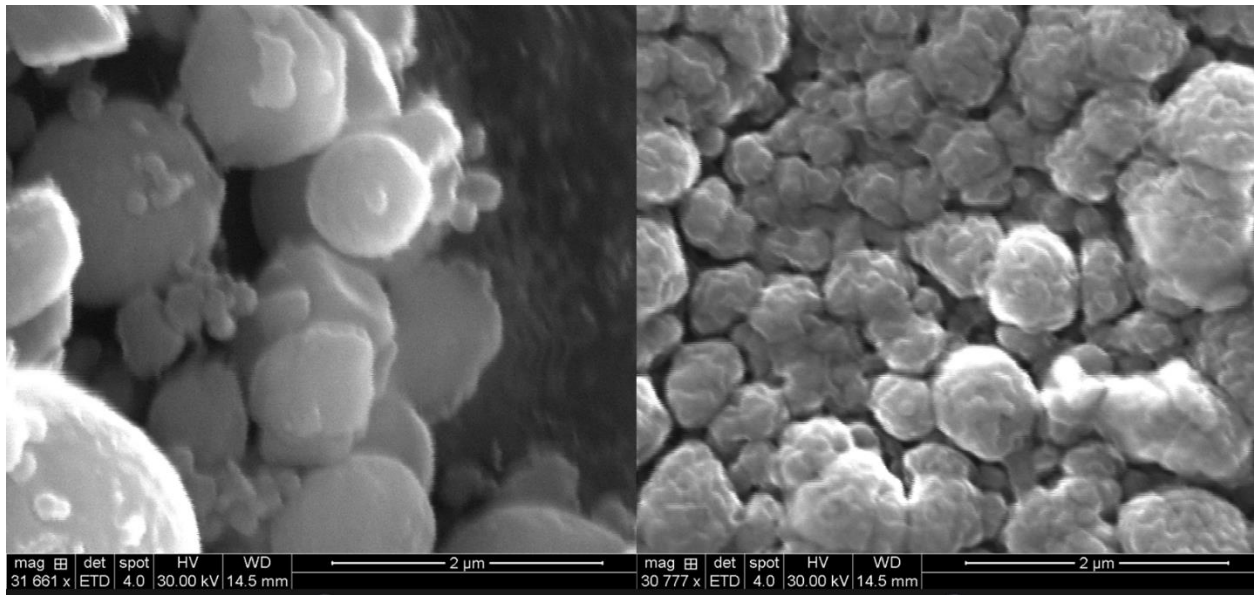
Figure 14. Cryo-EM images taken at approximately 31,000x with zero irradiation. Left: Control
(cyclohexane, water, no CNTs). Right: TiO_2-CNT Pickering emulsion

The droplets in the Control image are also larger, and appear more varied in size. The lack of

size consistency may be due to the absence of any stabilizing material.

7. References

[1] Jackson, R. B., Vengosh, A., Carey, J. W., Davies, R. J., Darrah, T. H., O'Sullivan, F., & Pétron, G. (2014). The Environmental Costs and Benefits of Fracking. *Annual Review of Environment and Resources*, *39*(1), 327–362. https://doi.org/10.1146/annurev-environ-031113-144051

[2] Nawaz, M., Miran, W., Jang, J., & Lee, D. S. (2017). Stabilization of Pickering emulsion with surface-modified titanium dioxide for enhanced photocatalytic degradation of Direct Red 80. *Catalysis Today*, *282*, 38–47. https://doi.org/10.1016/j.cattod.2016.02.017

[3] Lightowlers, R. J. (2015). Chemical pollution from fracking. *CHEM Trust*, 1-56.

[4] Tunsaringkarn, T., Siriwong, W., Rungsiyothin, A., & Nopparatbundit, S. (2012). Occupational Exposure of Gasoline Station Workers to BTEX Compounds in Bangkok, Thailand. *The International Journal of Occupational and Environmental Medicine*, *3*(3), 117-125. http://www.theijoem.com/ijoem/index.php/ijoem/article/view/133

[5] Han, F., Kambala, V. S. R., Srinivasan, M., Rajarathnam, D., & Naidu, R. (2009). Tailored titanium dioxide photocatalysts for the degradation of organic dyes in wastewater treatment: A review. *Applied Catalysis A: General*, *359*(1), 25–40. https://doi.org/10.1016/j.apcata.2009.02.043

[6] Rocha, O. R., Dantas, R. F., Duarte, M. M., & Silva, V. L. (2010). Oil Sludge Treatment by Photocatalysis Applying Black and White Light. *Chemical Engineering Journal, 157*(1), 80-85.

[7] Zhang, F. J., Liu, J., Chen, M.L., & Oh, W.C. (May 2009). Photoelectrocatalytic Degradation of Dyes in Aqueous Solution Using CNT/TiO$_2$ Electrode. *Journal of the Korean Ceramic Society*, 46(3), 263-270.

[8] Wu, W., Gao, S., Tu, W., Chen, J., & Zhang, P. (2010). Intensified photocatalytic degradation of nitrobenzene by Pickering emulsion of ZnO nanoparticles. *Particuology*, *8*(5), 453-457. https://doi.org/10.1016/j.partic.2010.05.006

[9] Nagaveni, K., Sivalingam, G., Hegde, M. S., & Madras, G. (2004). Solar photocatalytic degradation of dyes: high activity of combustion synthesized nano TiO$_2$. *Applied Catalysis B: Environmental, 48*(2), 83–93. https://doi.org/10.1016/j.apcatb.2003.09.013

[10] Zhai, W., Li, G., Yu, P., Yang, L., & Mao, L. (2013). Silver Phosphate/Carbon Nanotube-Stabilized Pickering Emulsion for Highly Efficient Photocatalysis. *J. Phys. Chem. C*, *117*(29),15183-15191.

[11] Hemalatha, K., Masthanaiah Ette, P., Madras, G., & Ramesha. K. (2015) Visible light assisted photocatalytic degradation of organic dyes on TiO$_2$–CNT nanocomposites. *J. of Sol-Gel Science and Technology. 73*(1), 72-82. https://link.springer.com/article/10.1007/s10971-014-3496-0

[12] Cunha, C., Panseri, S., Iannazzo, D., Piperno, A., Pistone, A., Fazio, M., & Galvagno, S. (2012). Hybrid composites made of multiwalled carbon nanotubes functionalized with Fe$_3$O$_4$ nanoparticles for tissue engineering applications. *Nanotechnology*, *23*(46), 465102. https://doi.org/10.1088/0957-4484/23/46/465102

[13] Luo, C., Tian, Z., Yang, B., Zhang, L., & Yan, S. (2013). Manganese dioxide/iron oxide/acid oxidized multi-walled carbon nanotube magnetic nanocomposite for enhanced hexavalent chromium removal. *Chemical Engineering Journal*, *234*, 256–265. https://ddoi.org/10.1016/j.cej.2013.08.084

[14] Saleh, N., Sarbu, T., Sirk, K., Lowry, G., Matyjaszewski, K., & Tilton, R. (2005). Oil-in-Water Emulsions Stabilized by Highly Charged Polyelectrolyte-Grafted Silica Nanoparticles. *Langmuir*, *21*, 9873-9878. https://pubs.acs.org/doi/abs/10.1021/la050654r

[15] Nakato, T., Ueda, H., Hashimoto, S., Terao, R., Kameyama, M., & Mouri, E. (2012). Pickering Emulsions Prepared by Layered Niobate $K_4Nb_6O_{17}$ Intercalated with Organic Cations and Photocatalytic Dye Decomposition in the Emulsions. *ACS Applied Materials & Interfaces*, *4*(8), 4338–4347. https://doi.org/10.1021/am300987x

[16] Gupta, V. K., Agarwal, S., & Saleh, T. A. (2011). Chromium removal by combining the magnetic properties of iron oxide with adsorption properties of carbon nanotubes. *Water Research*, *45*(6), 2207–2212. https://doi.org/10.1016/j.watres.2011.01.012

[17] Mishra, A. K., & Ramaprabhu, S. (2010). Magnetite Decorated Multiwalled Carbon Nanotube Based Supercapacitor for Arsenic Removal and Desalination of Seawater. *The Journal of Physical Chemistry C*, *114*(6), 2583–2590. https://doi.org/10.1021/jp911631w

[18] Ma, R., Wang, X., Huang, J., Song, J., Zhang, J., & Wang, X. (2017). Photocatalytic degradation of salicylic acid with magnetic activated carbon-supported F-N codoped TiO*2* under visible light. *Vacuum*, *141*, 157–165. https://doi.org/10.1016/j.vacuum.2017.04.003

[19] Das, D., Plazas-Tuttle, J., Venu Sabaraya, I., S. Jain, S., Sabo-Attwood, T., & B. Saleh, N. (2017). An elegant method for large scale synthesis of metal oxide–carbon nanotube nanohybrids for nano-environmental application and implication studies. *Environmental Science: Nano*, *4*(1), 60–68. https://doi.org/10.1039/C6EN00294C

[20] Fakhru'l-Razi, A., Pendashteh, A., Abdullah, L. C., Biak, D. R. A., Madaeni, S. S., & Abidin, Z. Z. (2009). Review of technologies for oil and gas produced water treatment. *Journal of Hazardous Materials*, *170*(2), 530–551. https://doi.org/10.1016/j.jhazmat.2009.05.044

[21] Metzger, L. (2016). 10 Billion Pounds of Chemicals Injected Underground in Texas for Fracking. Retrieved from https://environmenttexas.org/news/txe/10-billion-pounds-chemicals-injected-underground-texas-fracking

[22] Julkapli, N. M., Bagheri, S., & Hamid, S. B. A. (2014). Recent Advances in Heterogeneous Photocatalytic Decolorization of Synthetic Dyes. *The Scientific World Journal*. https://doi.org/10.1155/2014/692307

[23] Robinson, T., McMullan, G., Marchant, R., & Nigam, P. (2001). Remediation of dyes in textile effluent: a critical review on current treatment technologies with a proposed alternative. *Bioresource Technology*, *77*(3), 247–255. https://doi.org/10.1016/S0960-8524(00)00080-8

[24] Rajeshwari, K. V., Balakrishnan, M., Kansal, A., Lata, K., & Kishore, V. V. N. (2000). State-of-the-art of anaerobic digestion technology for industrial wastewater treatment. *Renewable and Sustainable Energy Reviews*, *4*(2), 135–156. https://doi.org/10.1016/S1364-0321(99)00014-3

[25] Adams, M., Campbell, I., & Robertson, P.K.J. (2008). Novel Photocatalytic Reactor Development for Removal of Hydrocarbons from Water. *International Journal of Photoenergy*, *2008*. https://doi.org/10.1155/2008/674537

[26] Linsebigler, A. L., Lu, G., & Yates, Jr., J. T. (1995). Photocatalysis on TiO_2 Surfaces: Principles, Mechanisms, and Selected Results. *American Chemical Society*, *95*(95), 735–758.

[27] Turchi, C. S., & Ollis, D. F. (1990). Photocatalytic degradation of organic water contaminants: Mechanisms involving hydroxyl radical attack. *Journal of Catalysis*, *122*(1), 178–192. https://doi.org/10.1016/0021-9517(90)90269-P

[28] Gaya, U. I., & Abdullah, A. H. (2008). Heterogeneous photocatalytic degradation of organic contaminants over titanium dioxide: A review of fundamentals, progress and problems. *Journal of Photochemistry and Photobiology C: Photochemistry Reviews*, *9*(1), 1–12. https://doi.org/10.1016/j.jphotochemrev.2007.12.003

[29] Frank, S. N., & Bard, A. J. (1977). Heterogeneous photocatalytic oxidation of cyanide and sulfite in aqueous solutions at semiconductor powders. *The Journal of Physical Chemistry*, *81*(15), 1484–1488.

[30] Kraeutler, B., & Bard, A. J. (1978). Heterogeneous photocatalytic preparation of supported catalysts. Photodeposition of platinum on titanium dioxide powder and other substrates. *Journal of the American Chemical Society*, *100*(13), 4317–4318. https://doi.org/10.1021/ja00481a059

[31] Chatterjee, D., & Dasgupta, S. (2005). Visible light induced photocatalytic degradation of organic pollutants. *Journal of Photochemistry and Photobiology C: Photochemistry Reviews*, *6*(2), 186–205. https://doi.org/10.1016/j.jphotochemrev.2005.09.001

[32] Sangkhun, W., Laokiat, L., Tanboonchuy, V., Khamdahsag, P., & Grisdanurak, N. (2012). Photocatalytic degradation of BTEX using W-doped TiO_2 immobilized on fiberglass cloth under visible light. *Superlattices and Microstructures*, *52*(4), 632–642. https://doi.org/10.1016/j.spmi.2012.06.026

[33] Murgolo, S., Petronella, F., Ciannarella, R., Comparelli, R., Agostiano, A., Curri, M. L., & Mascolo, G. (2015). UV and solar-based photocatalytic degradation of organic pollutants

by nano-sized TiO_2 grown on carbon nanotubes. *Catalysis Today*, *240*, 114–124. https://doi.org/10.1016/j.cattod.2014.04.021

[34] Aarthi, T., Narahari, P., & Madras, G. (2007). Photocatalytic degradation of Azure and Sudan dyes using nano TiO_2. *Journal of Hazardous Materials*, *149*(3), 725–734. https://doi.org/10.1016/j.jhazmat.2007.04.038

[35] Ray, A. K. (1999). Design, modelling and experimentation of a new large-scale photocatalytic reactor for water treatment. *Chemical Engineering Science*, *54*(15), 3113–3125. https://doi.org/10.1016/S0009-2509(98)00507-7

[36] Sauer, T., Cesconeto Neto, G., José, H. J., & Moreira, R. F. P. M. (2002). Kinetics of photocatalytic degradation of reactive dyes in a TiO_2 slurry reactor. *Journal of Photochemistry and Photobiology A: Chemistry*, *149*(1), 147–154. https://doi.org/10.1016/S1010-6030(02)00015-1

[37] Bolis, V., Busco, C., Ciarletta, M., Distasi, C., Erriquez, J., Fenoglio, I., & Morel, S. (2012). Hydrophilic/hydrophobic features of TiO_2 nanoparticles as a function of crystal phase, surface area and coating, in relation to their potential toxicity in peripheral nervous system. *Journal of Colloid and Interface Science*, *369*(1), 28–39. https://doi.org/10.1016/j.jcis.2011.11.058

[38] Li, Y., Zhang, W., Niu, J., & Chen, Y. (2012). Mechanism of Photogenerated Reactive Oxygen Species and Correlation with the Antibacterial Properties of Engineered Metal-Oxide Nanoparticles. *ACS Nano*, *6*(6), 5164–5173. https://doi.org/10.1021/nn300934k

[39] Sökmen, M., Allen, D. W., Akkaş, F., Kartal, N., & Acar, F. (2001). Photo-Degradation of Some Dyes using Ag-Loaded Titaniumdioxide. *Water, Air, and Soil Pollution*, *132*(1–2), 153–163. https://doi.org/10.1023/A:1012069009633

[40] Jung, K., Hong, J. S., Vittal, R., & Kim, K.-J. (2002). Enhanced Photocurrent of Dye-Sensitized Solar Cells by Modification of TiO_2 with Carbon Nanotubes. *Chemistry Letters*, *31*(8), 864–865. https://doi.org/10.1246/cl.2002.864

[41] O'Connell, M. J. (2006). *Carbon Nanotubes: Properties and Applications*. CRC Press.

[42] Iijima, S., & Ichihashi, T. (1993). Single-shell carbon nanotubes of 1-nm diameter. *Nature*, *363*(6430), 603–605. https://doi.org/10.1038/363603a0

[43] Ramoraswi, N. O., & Ndungu, P. G. (2015). Photocatalytic Properties of TiO_2 Supported on MWCNTs, SBA-15 and Silica-Coated MWCNTs Nanocomposites. *Nanoscale Research Letters*, *10*(427). https://doi.org/10.1186/s11671-015-1137-3

[44] Zhu, C.-L., Zhang, M.-L., Qiao, Y.-J., Xiao, G., Zhang, F., & Chen, Y.-J. (2010). Fe_3O_4/TiO_2 Core/Shell Nanotubes: Synthesis and Magnetic and Electromagnetic Wave Absorption Characteristics. *The Journal of Physical Chemistry C*, *114*(39), 16229–16235. https://doi.org/10.1021/jp104445m

[45] Jongnam, P., Eunwoong, L., Nong-Moon, H., Misun, K., Sung Chul, K., Yosun, H., & Taeghwan, H. (2005). One-Nanometer-Scale Size-Controlled Synthesis of Monodisperse Magnetic Iron Oxide Nanoparticles. *Angewandte Chemie*, *117*(19), 2932–2937. https://doi.org/10.1002/ange.200461665